

A comparison between two direct torque control strategies for flux and torque ripple reduction for induction motors drives

A. L. Mohamadein, Ragi A.R. Hamdy and Shady M. Gadoue

Electrical Eng. Dept., Faculty of Eng., Alexandria University, Alexandria, Egypt

This paper provides a comprehensive comparison of two high performance ripple reduction algorithms of Direct Torque Control (DTC) applied to induction motor drive. Viz., using a ripple minimization controller, which is based on torque slope calculation, and using a duty-cycle controller. Some drawbacks of the conventional DTC are the relatively large torque ripple, especially in the low speed region, and the variation of the switching frequency according to the amplitude of torque, and flux hysteresis bands and the motor speed. It is shown that the two proposed schemes improve the drive performance by combining a low torque ripple characteristics with fast torque dynamics while reducing the variation in the switching frequency. To verify the feasibility of the two schemes, numerical simulation and comparison with conventional DTC are carried out.

هذا البحث يعرض مقارنة متكاملة بين اثنتين من الخوارزميات لتقليل تناقض العزم لنظم التحكم المباشر في عزم المحركات الحثية. الخوارزم الأول يعتمد على حساب ميل العزم أما الثاني فيعتمد على التحكم في فترة التشغيل. من عيوب النظام التقليدي للتحكم المباشر في العزم التناقض في العزم خاصة عند السرعات البطيئة والتغير في تردد التقطيع الذي يعتمد على السرعة وحدود المتحكم التخلي. ولقد تم إثبات أن الخوارزمين المقترحين يعملان على تحسين الأداء من تقليل تناقض العزم مع سرعة في ديناميكية الأداء وتقليل التغير في تردد التقطيع. ولإتمام هذه الدراسة تم عمل نموذج للنظام للمقارنة بين الطريقة التقليدية وبين استخدام كل من الخوارزمين المقترحين. واستخدمت حزمة برامج ماتلاب – سميوليك للحصول على النتائج.

Keywords: Direct torque control, Torque ripple, Flux ripple, Ripples reduction

1. Introduction

In recent years different strategies for induction motor control are proposed, that offer dynamic torque control performance similar to that of the DC motors. Many strategies aimed to reduce the complexity of the flux orientation algorithms. The Direct Torque Control (DTC) technique has been recognized as a viable solution to achieve these requirements. However, it was accompanied with few drawbacks such as the large torque and current ripples, especially in the low speed region. Other reported disadvantages are the mismatching of mean output torque with the reference torque, and the variation of the switching frequency according to the motor operating speed, and the torque and flux hysteresis bands. To overcome these disadvantages low control sampling time (below $20\mu\text{s}$) is required [1-3]. The block diagram of the conventional DTC is shown in fig. 1.

Several studies have addressed the problem of improving the behavior of direct

torque controlled machines, especially by reducing the torque ripple and imposing the average switching frequency of the Voltage Source Inverter (VSI) [3].

D. Casadei et al. [4], proposed a control algorithm based on discrete space vector modulation (DSVM) technique that uses prefixed time intervals within a cycle period, i.e. by dividing the cycle period into three equal time intervals.

In this way, a higher number of voltage space vectors (19 vectors) can be synthesized with respect to the five available voltage vectors used in the basic DTC technique. This algorithm improves the torque and current ripple in the whole speed range but increases the inverter switching frequency which requires a discrete model of the machine valid for high sampling frequency. It also requires the definition of more accurate switching tables to select the voltage vector according to rotor position, and flux and torque errors.

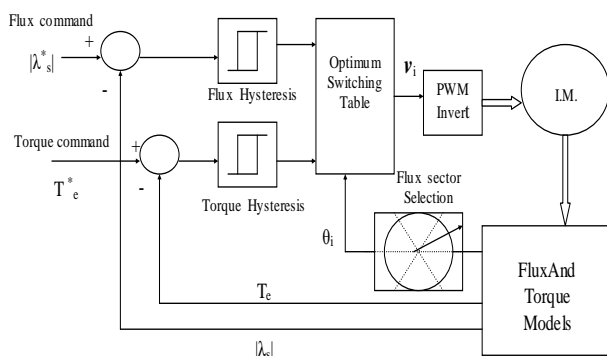


Fig.1. Conventional DTC scheme.

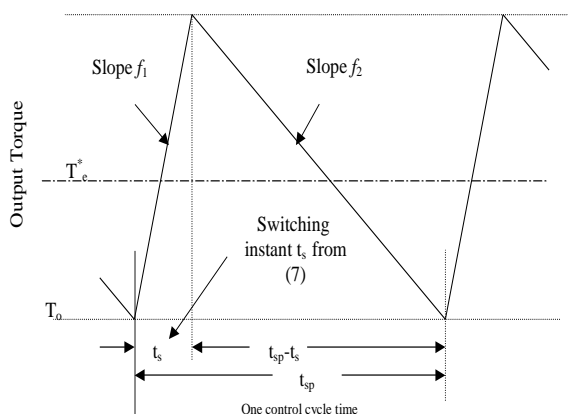


Fig. 2. Steady-state output torque waveforms by DTC.

L. Tang and M. Rahman [5], proposed another algorithm based on the mathematical model of the induction motor and space Vector Modulation Technique (SVM) instead of switching tables. This technique controls the slip frequency in each sampling interval so as to match the torque demand. The algorithm reduces both torque and flux ripples while maintaining constant switching frequency.

K. Lee et al. [6], presented another torque ripple reduction strategy using a three-level inverter to drive the induction motor with zero, half and full voltage levels, instead of the two-level inverter. The modification increases the number of available voltage vectors to 27, which reduces the torque ripple and maintains the switching frequency nearly constant. The appropriate selection of this voltage vector is more complex than in the two-level inverter.

Many other algorithms are proposed to overcome the problem of torque ripple and

variable switching frequency based on the improvement of the look-up tables and the variation of the torque controller hysteresis bandwidth [3].

In general, the proposed control strategies require complex control schemes, which erode the simplicity of DTC, or require high sampling rates in order to maintain effective control [3, 4].

Among different control strategies: two algorithms will be proposed due to their effectiveness and simplicity: Ripple minimization controller based on torque slope calculation and duty cycle control. The two algorithms reduce torque ripple while maintaining constant switching frequency [1, 2].

2. Induction motor model

The induction motor can be modeled with stator and rotor currents as the state variables by the following eqs. (7):

$$\begin{bmatrix} P i_{sd} \\ P i_{sq} \\ P i_{rd} \\ P i_{rq} \end{bmatrix} = \begin{bmatrix} a_{11} & a_{12}\omega + \omega_r & a_{13} & \omega a_{14} \\ -(a_{12}\omega + \omega_r) & a_{11} & -\omega a_{14} & a_{13} \\ a_{31} & -\omega a_{41} & a_{33} & \omega_s - a_{12}\omega \\ \omega a_{41} & a_{31} & a_{12}\omega - \omega_s & a_{33} \end{bmatrix}$$

$$\begin{bmatrix} i_{sd} \\ i_{sq} \\ i_{rd} \\ i_{rq} \end{bmatrix} + \begin{bmatrix} b_{11} & 0 \\ 0 & b_{11} \\ -b & 0 \\ 0 & -b \end{bmatrix} \begin{bmatrix} v_{sd} \\ v_{sq} \end{bmatrix}, \quad (1)$$

$$T_{em} = p L_{sr} (i_{rd} i_{sq} - i_{sd} i_{rq}), \quad (2)$$

$$\frac{\partial \omega}{\partial t} = \frac{p}{J} (T_{em} - T_l). \quad (3)$$

Where:

- R_s, R_r is the stator and rotor resistances,
- L_{ss}, L_{rr} is the stator and rotor equivalent Inductances,
- L_{sr} is the mutual inductance between stator and rotor,
- ω_s is the stator frequency in electrical rad/sec.
- ω_r is the rotor frequency in electrical rad/sec,
- p is the number of pole pairs, and

J Inertia constant.

$$a = \frac{1}{L_{SS}L_{rr} - L_{sr}^2}, a_{12} = aL_{SS}L_{rr},$$

$$b_{11} = aL_{rr}, a_{11} = -b_{11}R_s,$$

$$a_{33} = -aL_{SS}R_r, b = aL_{sr},$$

$$a_{13} = bR_r, a_{31} = bR_s,$$

$$a_{14} = bL_{rr}, a_{41} = bL_{SS}, \text{ and}$$

$$\omega_r = \omega_s - \omega.$$

3. Torque ripple in DTC

In principle, the DTC selects one of the six voltage vectors and two zero voltage vectors generated by a VSI in order to keep both the stator flux and the torque within their corresponding hysteresis bands. Application of this principle allows a decoupled control of flux and torque without the need of coordinate transformation, PWM pulse generation and current regulators. However, the presence of hysteresis controllers leads to a variable switching frequency operation. In addition, the limited number of available voltage vectors determines the presence of current and torque ripple with variable frequencies particularly at low speed.

The electromagnetic torque in an induction machine can be written as [2]:

$$T_{em} = \frac{3}{2} P \frac{L_{sr}}{\sigma L_{SS} L_{rr}} |\lambda_r| |\lambda_s| \sin(\gamma). \quad (4)$$

Where:

λ_s, λ_r are stator and rotor flux linkage.

γ is the torque angle, and

σ is the leakage coefficient $\sigma = \frac{1 - L_{sr}^2}{L_{SS}L_{rr}}$.

The change of torque over an arbitrary time period t is given by:

$$\partial T_{em} = \frac{3}{2} P \frac{L_{sr}}{\sigma L_{SS}L_{rr}} |\lambda_r| |\lambda_s| \left(\sin\left(\gamma(t_o) + \frac{d\gamma}{dt} t\right) - \sin(\gamma(t_o)) \right). \quad (5)$$

Where (in the stator-flux-oriented reference frame):

$$\frac{d\gamma}{dt} = \omega_s - \omega_r \text{ and } \omega_s = \frac{v_{sq} - R_s i_{sq}}{\lambda_{sd}}. \quad (6)$$

In DTC, the flux is divided into six 60° sectors allowing selection of the appropriate voltage vector. Selecting the suitable voltage vectors moves the flux in the desired direction and controls the stator flux magnitude. Torque can be increased (decreased) by selecting a voltage vector that will increase (decrease) the magnitude of the quadrature component of the stator flux relative to the rotor flux. The effect of this voltage vector on the rate of torque change can be calculated from eqs. (5) and (6). As the selected voltage-vector is applied for the full sampling period (i.e. 100% duty cycle), the resulting increase in torque; when a non-zero voltage-vector is applied; becomes significantly higher than the decrease in torque when a zero voltage-vector is applied. This is particularly at low frequencies, resulting in a large torque ripple and reduced switching frequency [2, 4, 8].

4. Torque ripple reduction using torque slope equation

The torque ripple reduction using torque slope equation technique has the advantage of minimizing the torque ripple meanwhile maintaining constant switching frequency. The output voltage vector v_s is selected using the conventional DTC switching table, while the pulse duration (duty cycle) of v_s is determined by the minimum torque-ripple condition. The instantaneous torque variation of the motor can be expressed as a function of the applied voltage vector v_s . Hence, the rms torque-ripple equation during one switching period can be obtained from the instantaneous torque variation equations. The optimal switching instant t_s (the on duration of v_s) is determined by having partial derivative of the rms torque ripple equation with respect to t_s [1]. Through which the optimal switching instant t_s for minimum torque ripple can be written as [1]:

$$t_s = \frac{2(T_e^* - T_0) - f_2 t_{sp}}{(2f_1 - f_2)} \quad (7)$$

Where:

- T_e^* is the torque command,
- T_0 is the torque initial value,
- f_1 is the slope of torque variation by the non-zero voltage vector,
- f_2 is the slope of torque by the zero voltage vector, and
- t_{sp} is the control sampling time.

The control block diagram of the proposed method is shown in fig. 3. The stator and rotor flux linkages are calculated from the voltage and current models of the induction motor. The proposed controller combines the voltage vector selection block of the conventional DTC with the minimum torque-ripple controller which regulates the turn-on duration of the active voltage-vector by inserting a zero voltage-vector at $t = t_s$. The basic switching vector selection rule is the same as that of the conventional methods. The flow chart of the proposed strategy is shown in fig. 4.

5. torque ripple reduction using duty-cycle controller

To address the problem of torque ripple and variable switching frequency, a duty-cycle controller is introduced to the conventional DTC architecture. It controls the average torque increase when a non-zero voltage vector is applied to match the torque decrease when a zero voltage vector is applied.

Consider the operation of DTC where the scheme is used to control the average output torque to be equal to the lower hysteresis limit

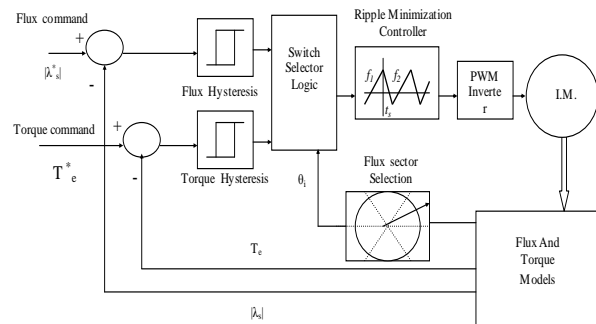


Fig. 3. DTC with torque ripple minimization controller.

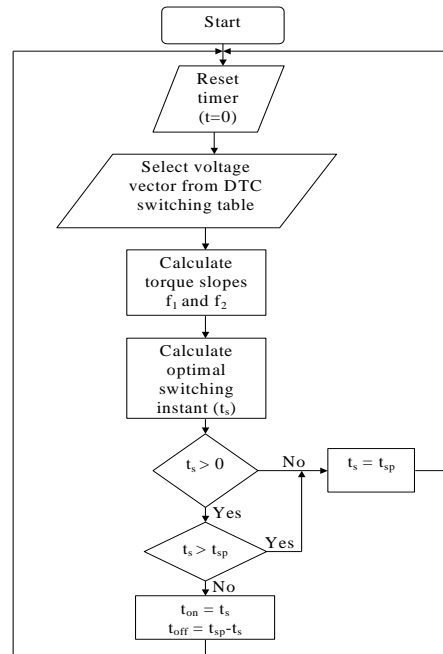


Fig. 4. Flow chart of the proposed strategy.

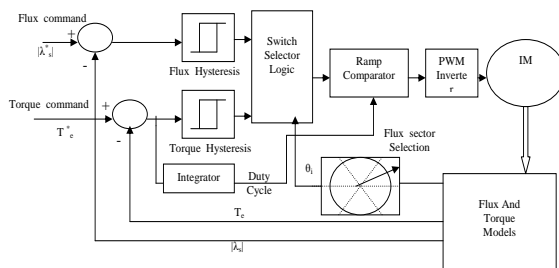


Fig. 5. DTC with Duty-cycle controller.

and the torque is allowed to decay naturally. If the duty cycle is correct and the average torque increase matches the average torque decrease, then the mean torque matches the lower hysteresis limit. If the duty cycle is too long, then the average torque increase will be higher than the average torque decrease, and the mean torque will become higher than the hysteresis limit. If the duty cycle is too short, then the average torque increase will be too low, and the mean torque will become lower than the hysteresis limit. By varying the duty cycle to control the average output torque to be equal to the lower hysteresis limit, the conditions for reduced torque ripple will be met [6]. The block diagram of the proposed

system is shown in fig. 5 where the torque error drives an integrator that adjusts the duty cycle and the lower hysteresis limit is set to be equal to the torque reference. Fig.6 shows the steady-state operation of the duty-cycle controller.

6. Simulation results and comparison

Three Matlab/Simulink models were developed to examine the different control algorithms; conventional DTC, DTC using torque ripple minimization controller, and DTC with

duty-cycle controller. The parameters of the induction motor are shown in Appendix A.

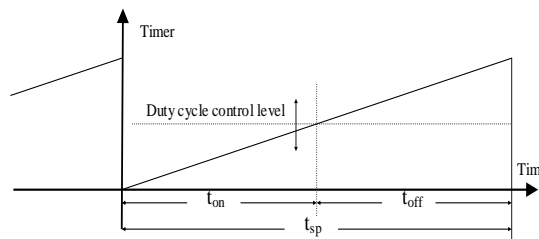


Fig. 6. Duty cycle control of space voltage vector.

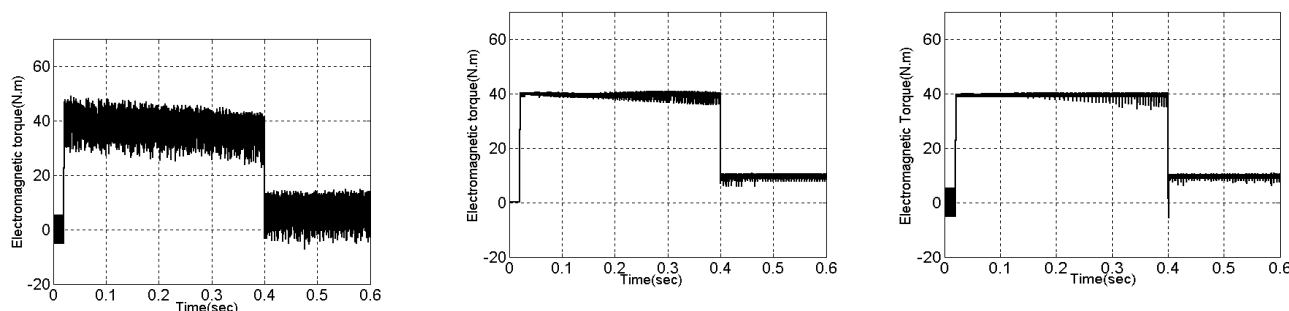


Fig. 7. Electromagnetic Torque (a) conventional DTC (b) DTC with ripple minimization controller (c) DTC with duty-cycle controller.

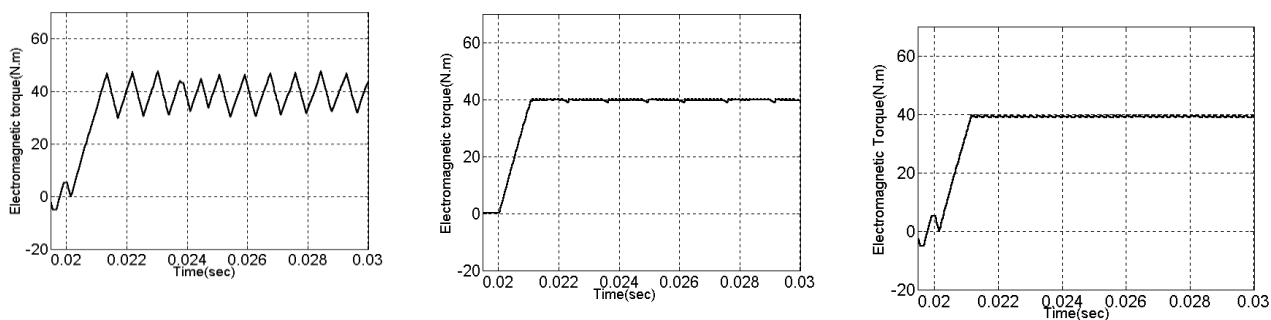


Fig. 8. Low-speed performance (a) conventional DTC (b) DTC with ripple minimization controller (c) DTC with duty-cycle controller.

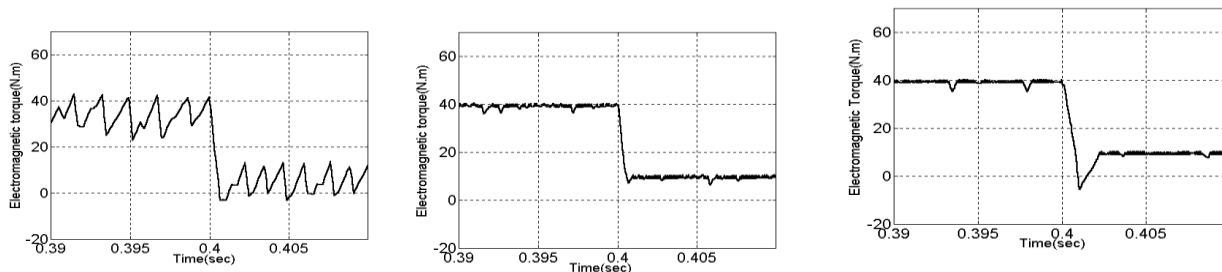


Fig.9. High-speed performance (a) conventional DTC (b) DTC with ripple minimization controller (c) DTC with duty-cycle controller.

A step torque command of 40 Nm (rated torque) is applied to the induction motor at 0.02sec then changed to 10N.m at 0.04sec when the machine speed reaches 1000rpm. The system is simulated with controller sampling time fixed to 120 μ s, flux hysteresis band set to $\pm 0.5\%$ of rated flux, and torque hysteresis band set to $\pm 1\%$ of rated torque at steady state speed of 1000rpm and the following results are obtained:

6.1. Torque control performance

Fig. 7 shows the electromagnetic torque in the three cases when the step torque command is applied to the induction motor at a steady-state speed of 1000rpm.

By comparing the output torque response in the three cases, the conventional DTC has a peak to peak torque ripple over 17N.m fig. 7-a, where the DTC with torque ripple minimization control (first method) reduces the torque ripple to an average of 2.5N.m fig. 7-b, while the DTC with duty cycle controller reduces it to an average of 2N.m fig. 7-c. The poor torque control capability of the conventional DTC, in particular, in the low speed region, is caused by a relatively large slope f_1 , i.e., low back EMF in that region.

The torque step rising times for the three cases are nearly the same (1.2msec). The low speed performance is shown in fig. 8 where the torque ripple is reduced at starting from 17N.m in conventional case to 0.7N.m in the first case and to 0.8N.m in the second case.

Fig. 9 shows the drive performance in the high-speed region when the motor torque command steps from 40N.m to 10N.m. Simulation results show that the three algorithms have a step falling time of around 0.6msec. In the second controller, the torque has an overshoot as the conventional DTC. This is due to the large torque error that saturates the duty cycle integrator and the system acts as conventional DTC at this moment.

In the conventional DTC, the mean output torque is 36N.m for a torque command of 40N.m and 7N.m for a torque command of 10N.m. The first method enhances the response by raising the mean output torques to 38N.m and 9N.m respectively. The duty-cycle controller further enhances the steady state

performance having mean output torques of 39.5N.m and 9.5N.m, respectively.

The first controller has good performance in terms of torque control characteristic, particularly, in the low speed region as shown in fig. 8-b. This is because at the beginning, a selected active voltage vector is fully turned on during the entire control time period ensuring rapid torque build-up.

The duty cycle decreases rapidly to below tens of microseconds because f_1 is larger than f_2 in the low speed region. Torque ripple increases in the high-speed region as shown in fig. 9-b. This is because f_2 increases in proportion to the motor speed, while f_1 is less dependent of the motor speed but it is strongly affected by the selected voltage vectors [1]. Torque slopes f_1 , f_2 and the optimal switching instant t_s are shown in fig. 10.

The results obtained by the duty-cycle controller are similar to those of the ripple minimization controller. The controller reduces the torque ripple particularly in the low speed region. In addition the duty-cycle controller maintains the mean output torque to be equal to the command torque.

Conventional DTC is characterized by a variable switching frequency according to the motor speed and the hysteresis bands of torque and flux. First control method achieves constant switching frequency regulation. Duty-cycle controller also reduces the variation in the switching frequency.

The reduction in the torque ripple is associated with a corresponding reduction in the phase current ripple in the whole speed range for both algorithms. Fig. 11 shows the response of the phase current in the three cases over the whole speed range.

6.2. Flux control performance

The control performance of the stator flux is shown in fig. 12 and fig. 13. The induction machine is running at a steady-state speed of around 1000rpm, and the stator flux is regulated at the rated value of 0.42wb assuming that the operation of the drive is considered after the flux build-up mode where torque ripple minimization is not needed.

Conventional DTC has a stator flux ripple of 0.06wb. Both schemes reduce the stator

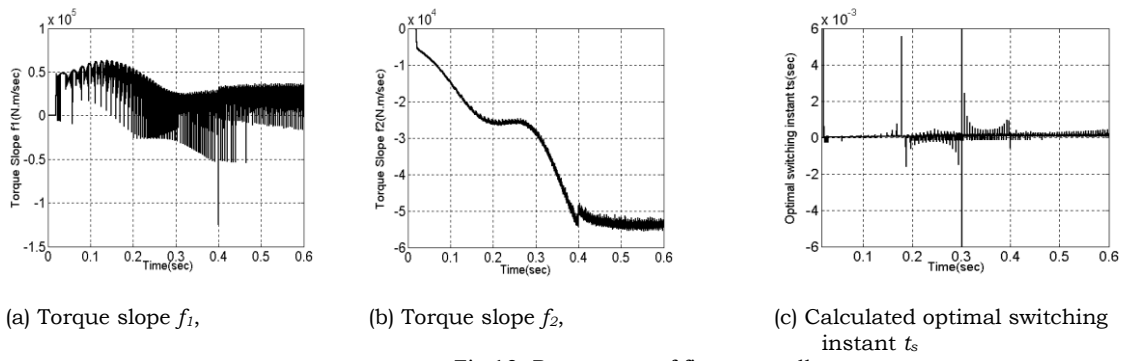


Fig.10. Parameters of first controller.

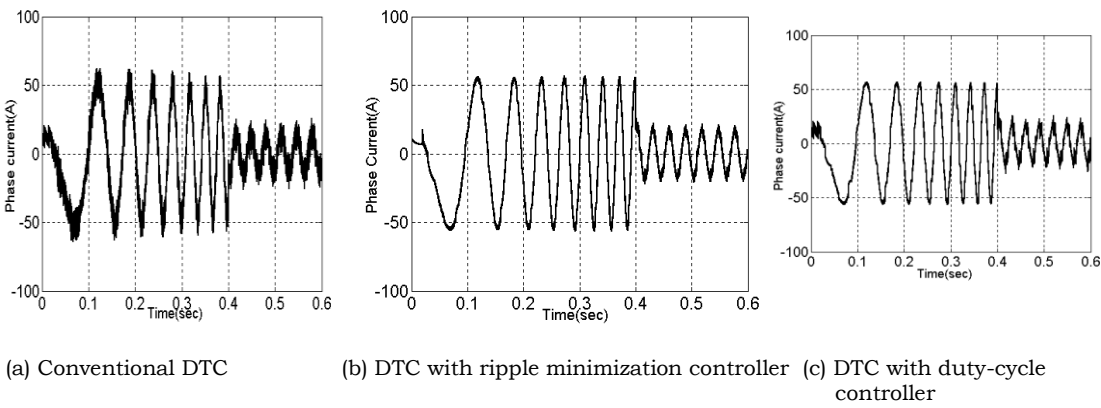


Fig.11. Phase current.

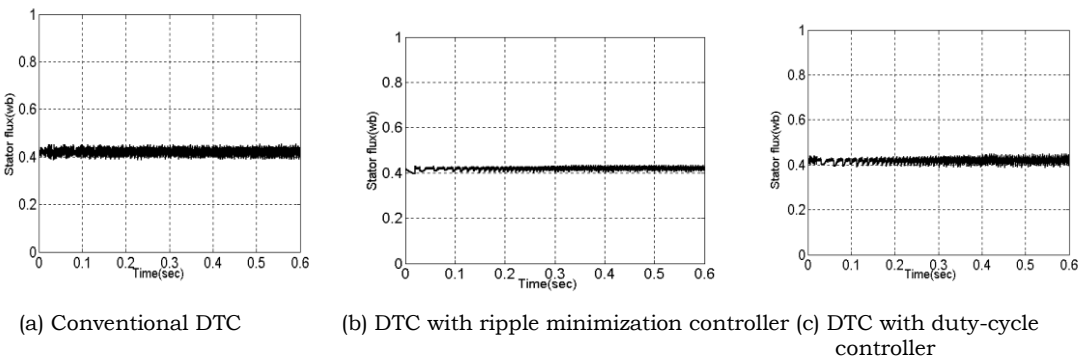


Fig.12. Stator flux.

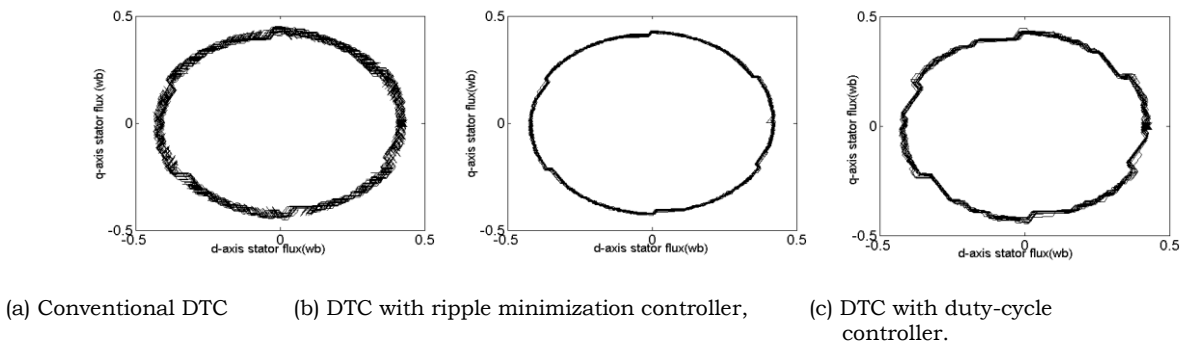


Fig.13. Trajectory of d- and q- axes stator flux.

flux ripple. The first controller controls the switching instant of the voltage vector focusing on the minimum torque ripple condition in eq. (7), therefore the flux control may be different from the conventional method. The flux ripple is reduced to 0.02wb. The duty-cycle controller reduces the flux ripple since a zero voltage vector is inserted in each control cycle according to the duty-cycle that affects the stator flux control. The flux ripple is reduced to 0.05wb.

As a conclusion, the results above verify that the two proposed control methods reduce the torque ripple significantly without deteriorating the flux control capability. Flux ripple reduction by the first method is superior to the second method.

7. Conclusions

In this paper two proposed control techniques to reduce torque ripples and regulate the switching frequency are investigated. Both strategies managed to fix the switching frequency. It should be noted that the higher the switching frequency the better the controller performance, however this will increase the switching losses and require fast semiconductor switches. Both strategies show different capabilities in torque and flux ripples reductions.

In the first technique, the optimal switching instant is calculated at each switching cycle to satisfy the ripple minimum condition based on the instantaneous torque slope equations. The scheme has been shown to reduce torque ripple while maintaining constant switching frequency. In the second technique, duty-cycle of the voltage vector is controlled in each control cycle. The scheme shows to reduce torque ripple particularly at low speed range. It shows good capabilities in controlling the mean output torque and limiting the switching frequency variation. Simulation results verify that the two proposed techniques improve the torque control characteristic without deteriorating the flux control capability.

Appendix A

Parameters of the induction motor

Rated output power	10 hp
Rated line voltage	220 V
Number of poles	4
Base speed	1750 rpm
Rated torque	40 N.m
Stator resistance (R_s)	0.15 Ω
Rotor resistance (R_r)	0.17 Ω
Stator leakage inductance (L_{ss})	0.035 H
Rotor leakage inductance (L_{rr})	0.035 H
Mutual inductance (L_{sr})	0.0338 H
Load inertia (J)	0.14 kg-m ²

References

- [1] Jun-Koo Kang, Seung-Ki Sul, "New Direct Torque Control of Induction Motor for Minimum Torque Ripple and Constant Switching Frequency", IEEE Transactions on Industry Applications, Vol. 35 (5) (1999).
- [2] D. Telford, M. W. Dunnigan, and B. W. Williams, "A Novel Torque-Ripple Reduction Strategy for Direct Torque Control", IEEE Transaction industrial electronics, Vol. 48 (4) (2001).
- [3] Carlos A. Martins, Xavier Roboam, Thierry A. Meynard, and Adriano S. Carvalho, "Multi-Level Direct Torque Control with Imposed Switching Frequency and Reduced Ripple", Power Electronics Specialists Conference, 2000, PESC 00. 2000 IEEE 31st Annual , Vol. 1, pp. 435-441 (2000).
- [4] D. Casadei, G. Serra and A. Tani, "Implementation of Direct Torque Control Algorithm for Induction Motors Based on Discrete Space Vector Modulation", IEEE Transaction Power Electronics, Vol. 15 (4), (2000).
- [5] L. Tang and M. Rahman, "A New Direct Torque Control Strategy for Flux and Torque Ripple Reduction for Induction Motor Drives-A Matlab/Simulink Model", International Electrical machines and drives Conference, IEMDC 2001, IEEE International, 2001, pp. 884-890 (2001).
- [6] Song, Ick Choy, Joo-Yoep Choi, Jae-Hak Yoon and Se-Hyun Lee, "Torque Ripple

Reduction in DTC of Induction Motor Driven by 3-level Inverter with Low Switching Frequency”, Power Electronics Specialists Conference, 2000. PESC 00, 2000 IEEE 31st Annual, Vol. 1, pp. 448-453, (2000).

- [7] R. Hamdy, “Doubly Fed Induction Motor Simulation and Control”, M. Sc Thesis,

Faculty of Engineering, Alexandria University (1994)

- [8] Takahashi and T. Noguchi, “A new quick response and high efficiency control strategy of an induction motor”, IEEE Transactions on Industry applications, Vol. IA-22 (5) (1986).

Received June 21, 2003

Accepted September 30, 2003